10.1071/CH20210_AC

Australian Journal of Chemistry 2021, 74(1), 34-47

Supplementary Material

Copper Complexes of Benzoylacetone bis-Thiosemicarbazones: metal and ligand based redox reactivity.

Jessica K. Bilyj,[A] *Jeffrey R. Harmer*[B] *and Paul V. Bernhardt*[A,C]

[A] *School of Chemistry and Molecular Biosciences, University of Queensland, Brisbane, Qld 4072, Australia*

[B] *Centre for Advanced Imaging, University of Queensland, Brisbane, Qld 4072, Australia*

[C] *Corresponding author. Email: p.bernhardt@uq.edu.au*

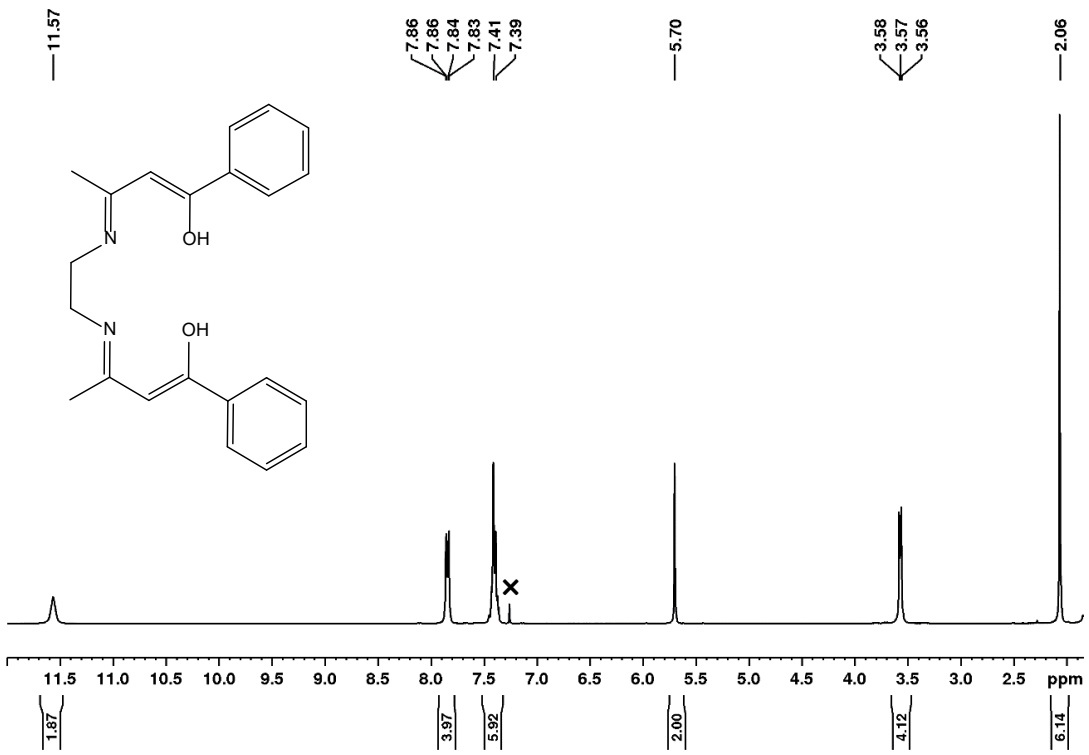

Fig. S1 ^{1}H NMR spectrum of Proligand 1 in $CDCl_3$. Solvent peaks indicated with ×.

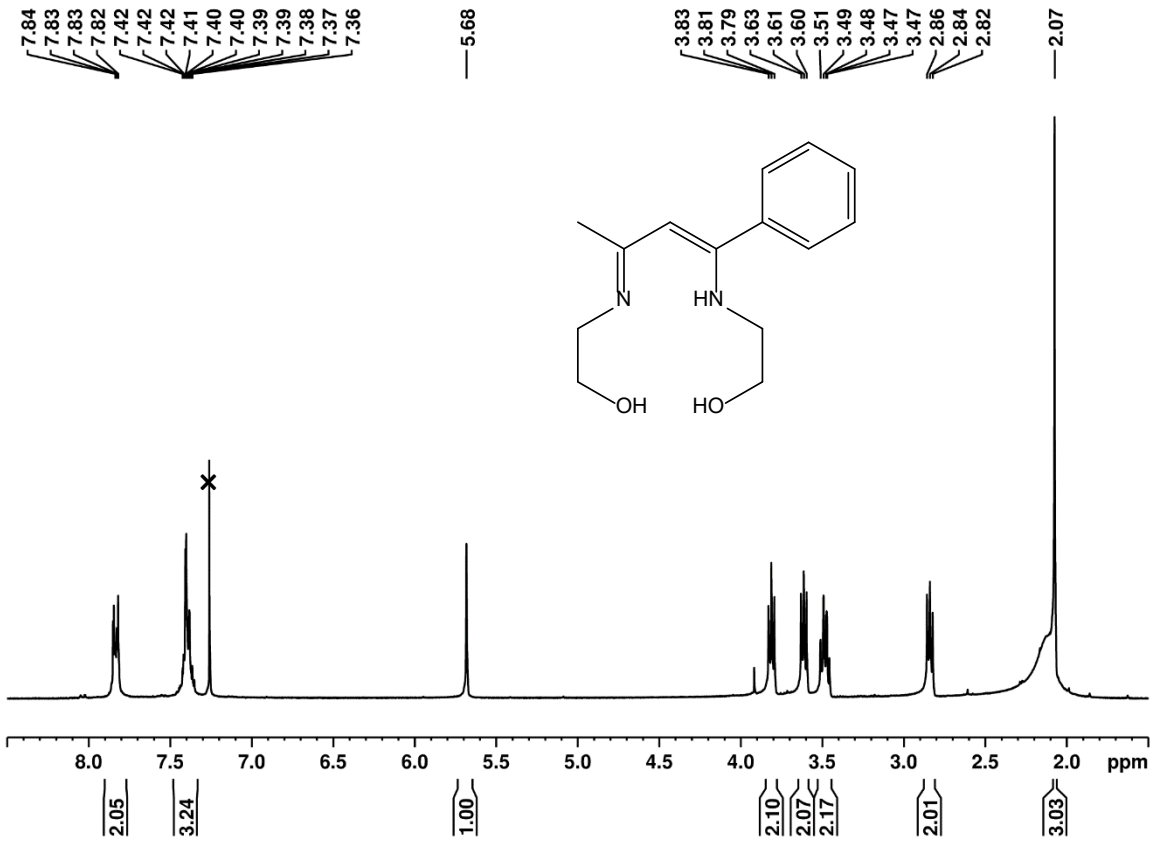

Fig. S2 ^{1}H NMR spectrum of Proligand 2 in $CDCl_3$. Solvent peaks indicated with ×.

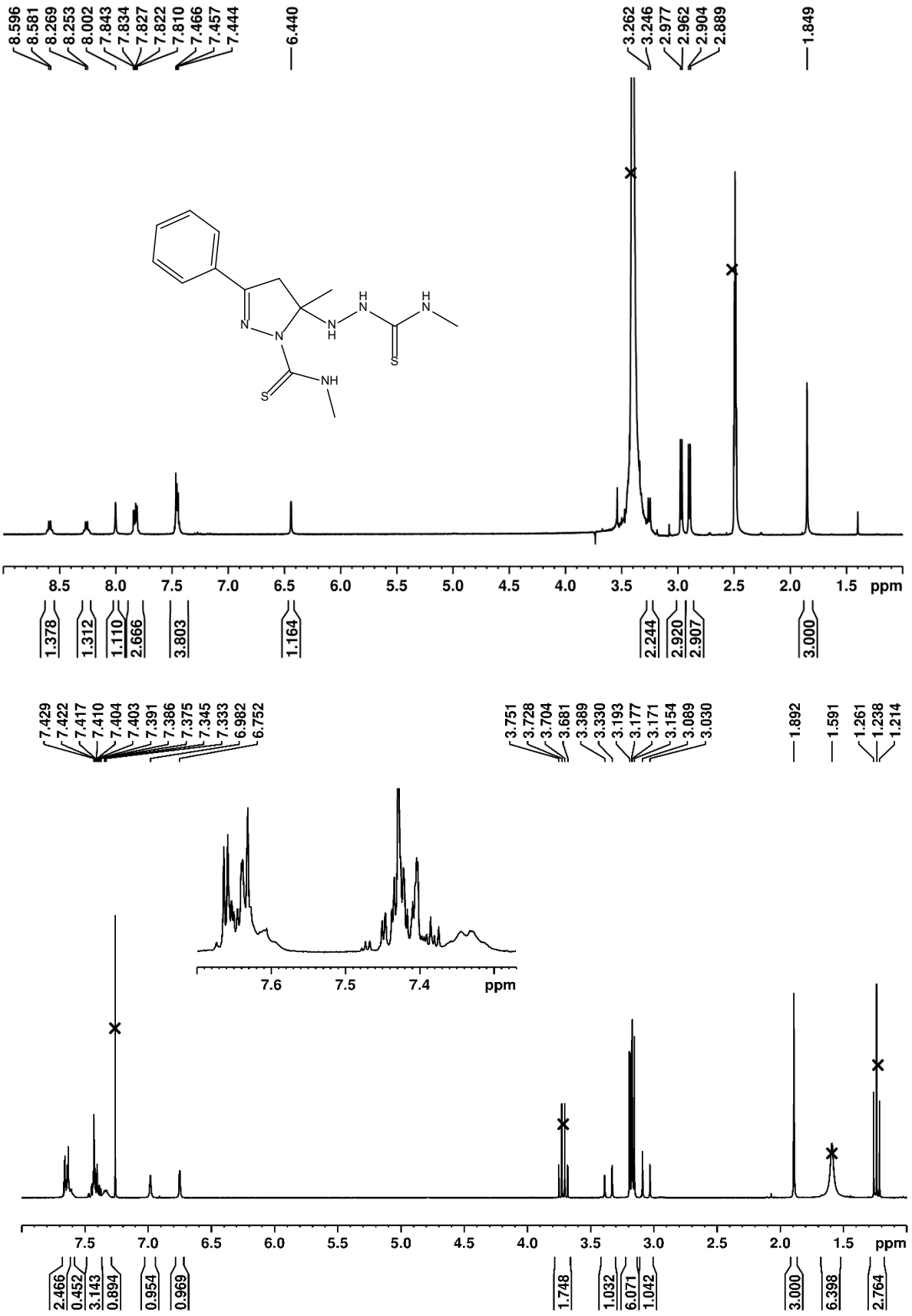

Fig. S3 ^{1}H NMR spectrum of H_3banme in DMSO-d (above) and $CDCl_3$ (below).Solvent peaks indicated with × including EtOH.

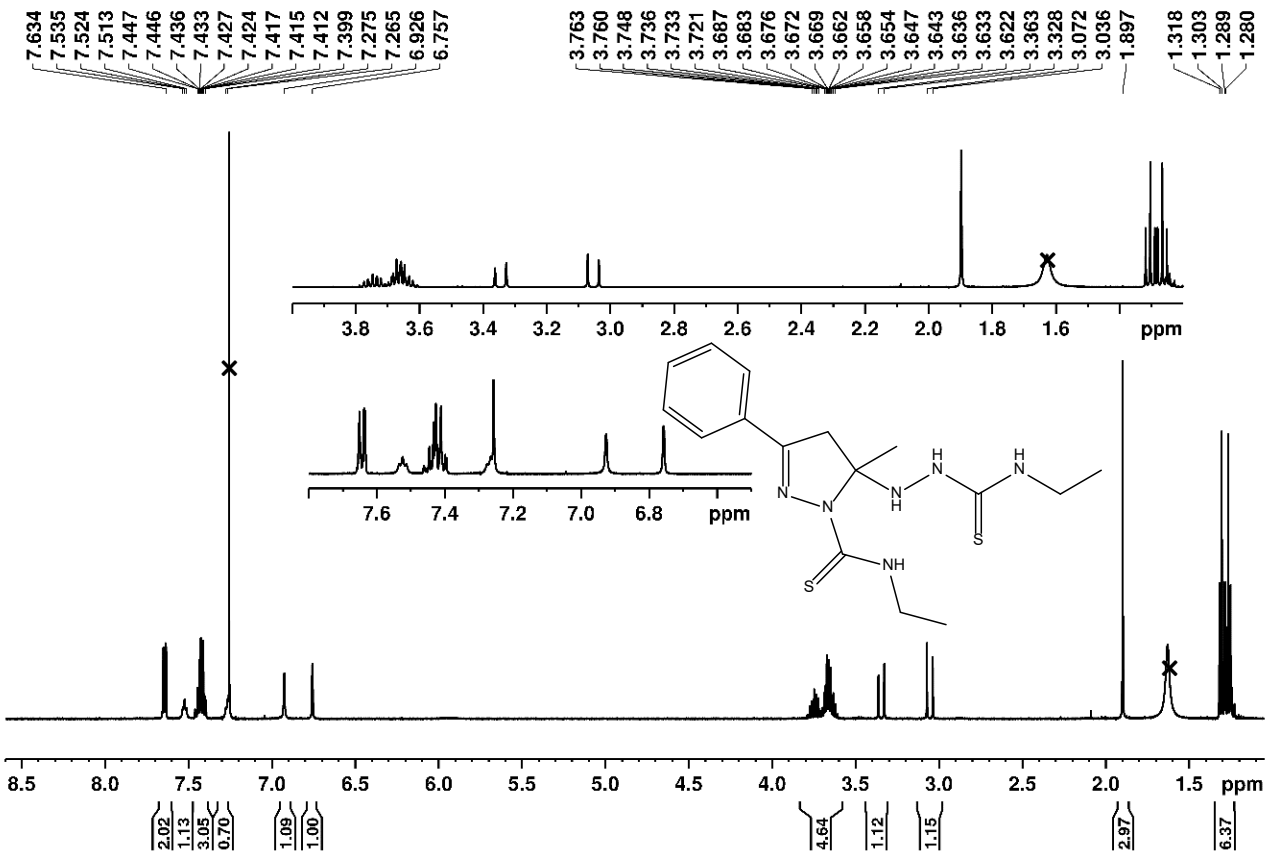

Fig. S4 ^{1}H NMR spectrum of H_3banet in $CDCl_3$.Solvent peaks indicated with ×.

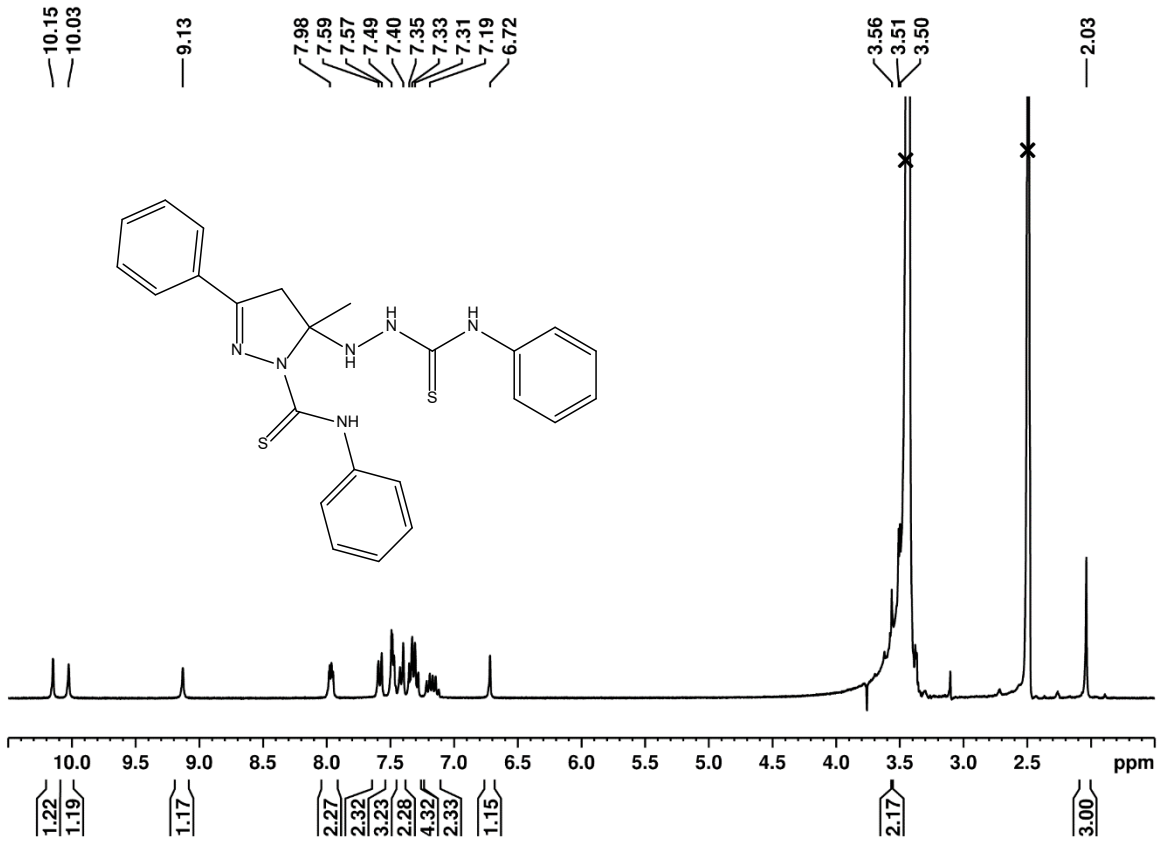

Fig. S5 ^{1}H NMR spectrum of H_3banphe in DMSO-d_6.Solvent peaks indicated with ×.

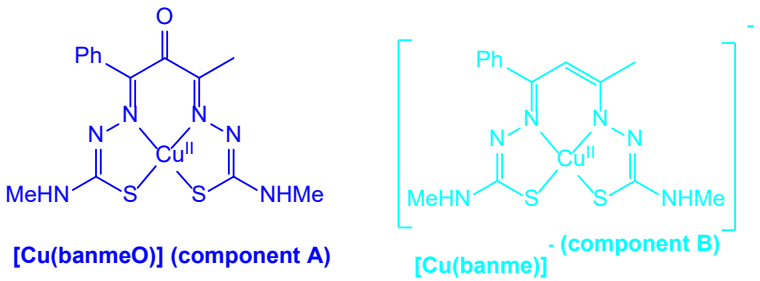

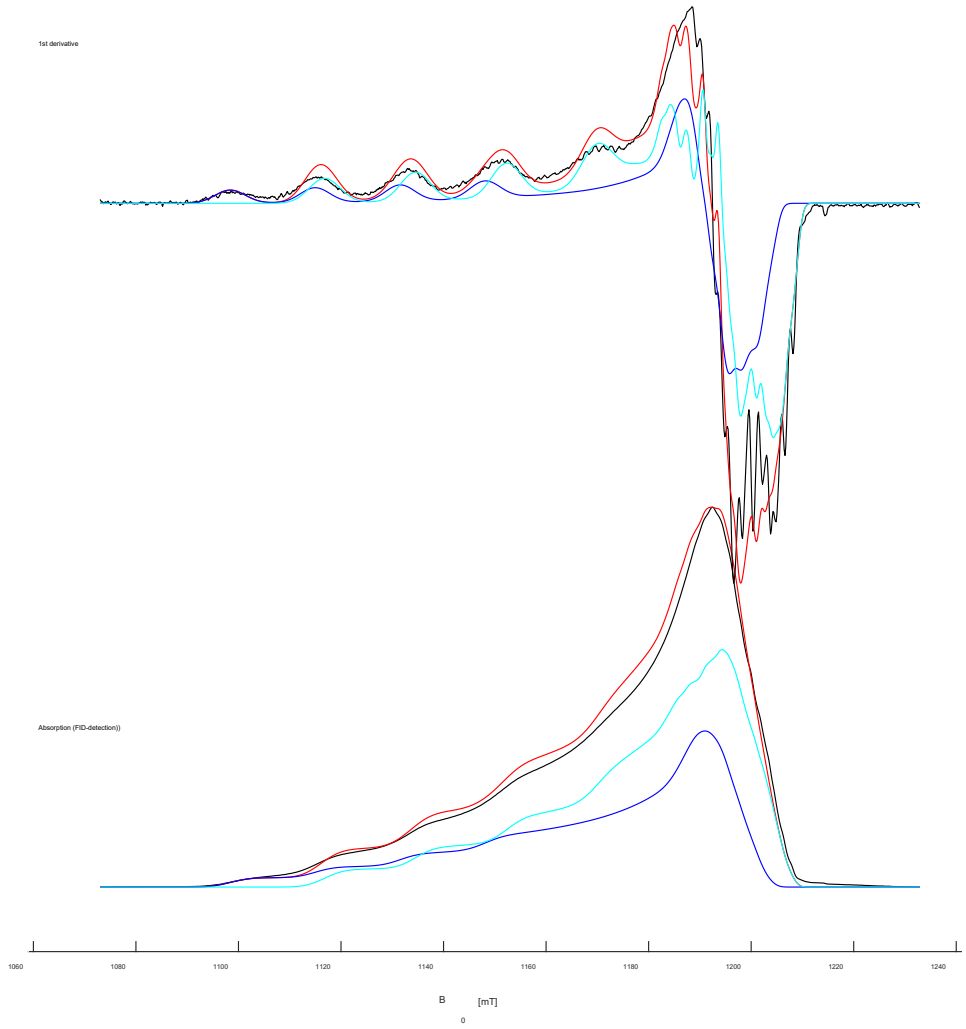

Fig. S6. Q-band FID-detect field-sweep EPR of $[Cu(banme)]^-$ (anaerobic) at 30 K. Experimental (black), simulation total (red): component A (blue) and component B (cyan). Spin Hamiltonian parameters: component A (40%) g_x 2.0248, g_y 2.0357, g_z 2.158; $A_{Cu,x}$ (MHz) 79, $A_{Cu,y}$ 50, $A_{Cu,z}$ 490; $A_{N,x,y,z}$ 41.9; linewidths (x, y and z) 65, 65 and 120 MHz and component B (60%) g_x 2.0165 , g_y 2.037, g_z 2.120; $A_{Cu,x}$ 50, $A_{Cu,y}$ 70, $A_{Cu,z}$ 515]; $A_{N,x,y,z}$ 41.9.; linewidths (x, y and z) 40, 40 and 160 MHz. N.B. unit conversion A (cm^{-1}) = 0.33356×10^{-4} A (MHz).

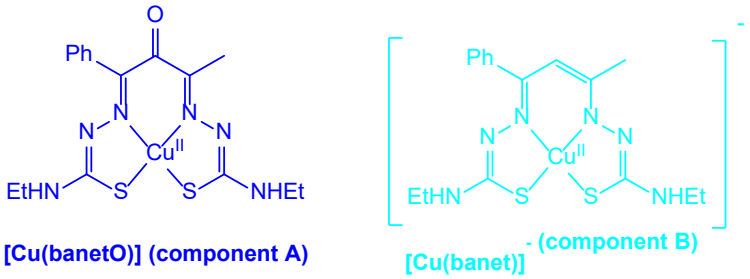

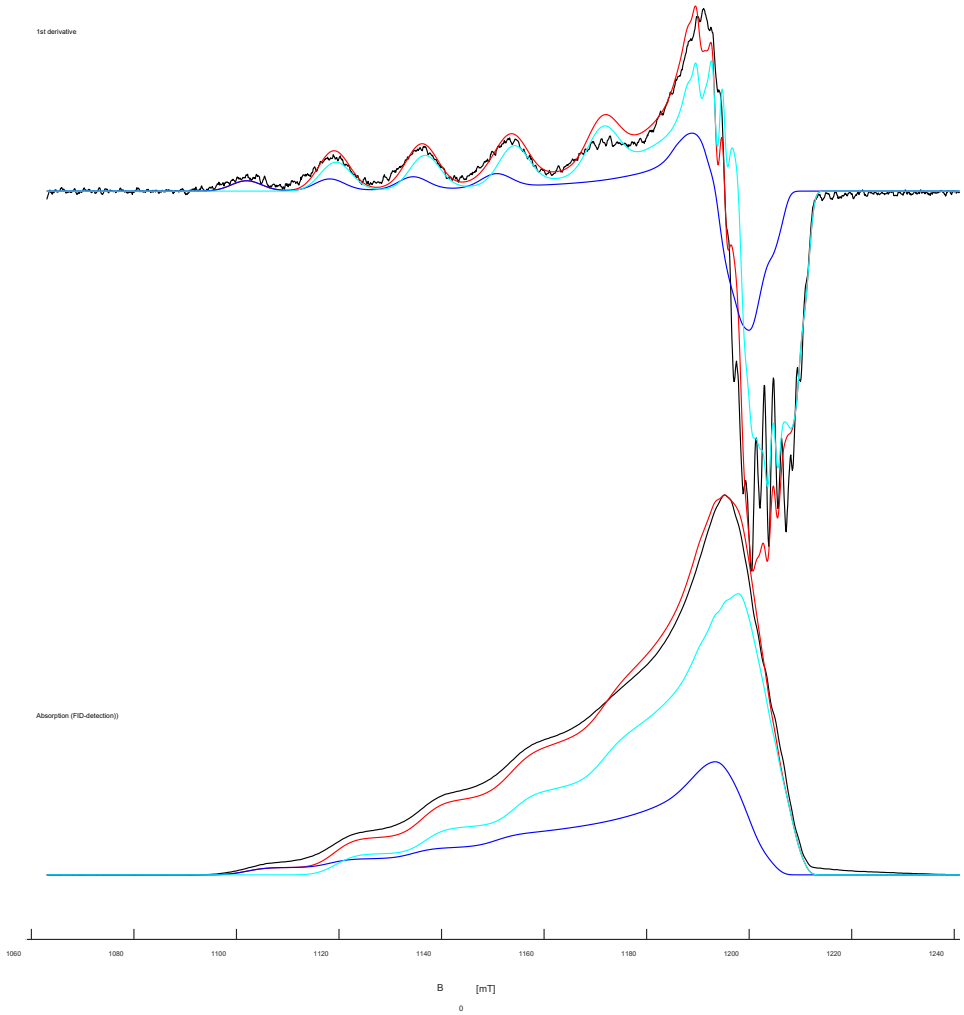

Fig. S7. Q-band FID-detect field-sweep EPR of $[Cu(banet)]^-$ (anaerobic) at 30 K. Experimental (black), simulation total (red): component A (blue) and component B (cyan). Spin Hamiltonian parameters: component A (30%) g_x 2.0248, g_y 2.0365, g_z 2.157; $A_{Cu,x}$ (MHz) 59, $A_{Cu,y}$ 59, $A_{Cu,z}$ 480; $A_{N,x,y,z}$ 41.9; linewidths (x, y and z) 65, 65 and 120 MHz and component B (70%) g_x 2.0165 , g_y 2.034, g_z 2.121; $A_{Cu,x}$ 50, $A_{Cu,y}$ 50, $A_{Cu,z}$ 505]; $A_{N,x,y,z}$ 41.9; linewidths (x, y and z) 40, 40 and 160 MHz.

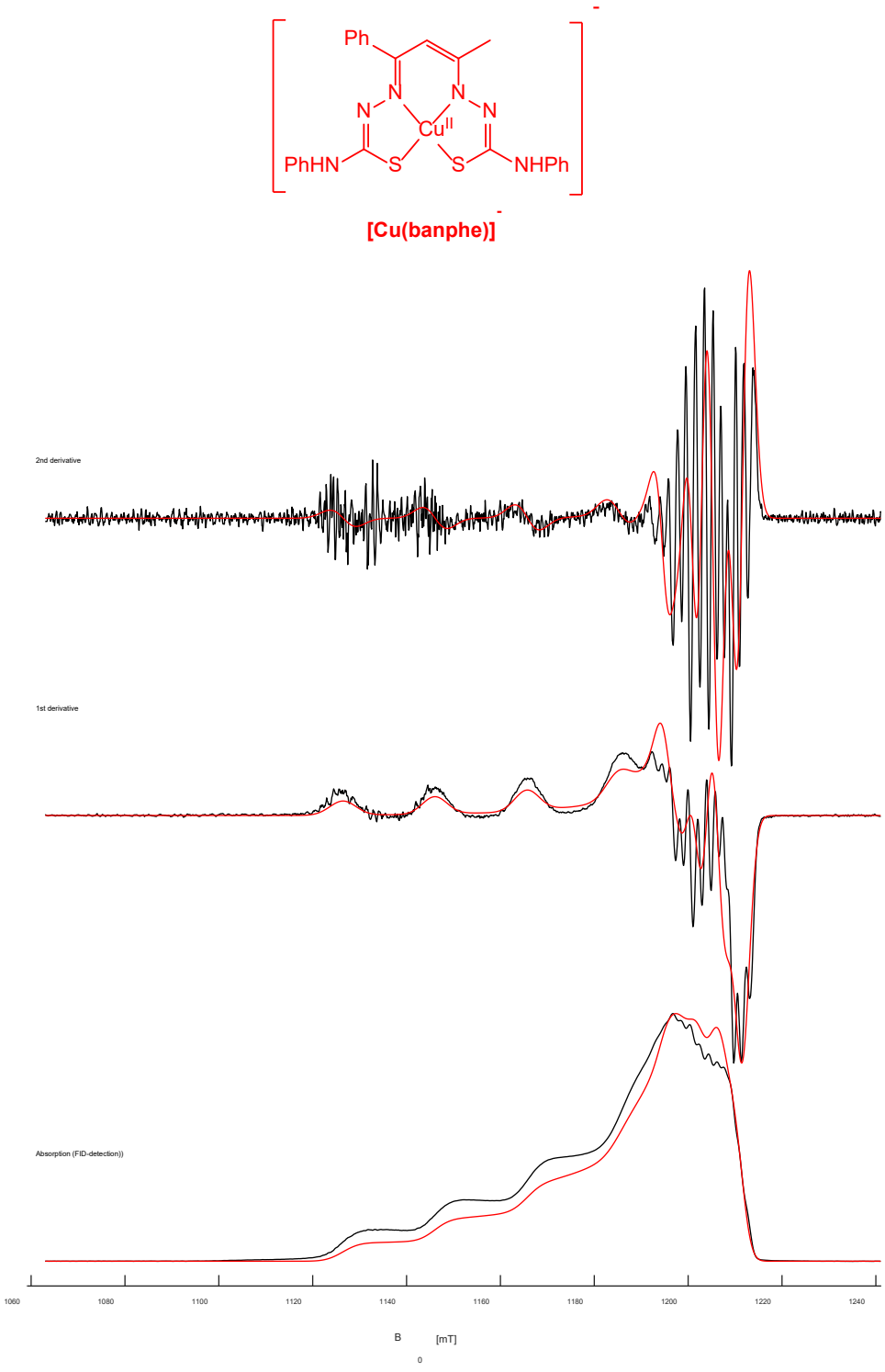

Fig. S8. Q-band FID-detect field-sweep EPR of $[Cu(banphe)]^-$ (anaerobic) at 30 K. Experimental (black) and simulation (red). Spin Hamiltonian parameters: g_x 2.0161, g_y 2.0229, g_z 2.1015; $A_{Cu,x}$ (MHz) 116, $A_{Cu,y}$ 93, $A_{Cu,z}$ 565; $A_{N,x,y,z}$ 41.9; linewidths (x, y and z) 30, 30 and 50 MHz.

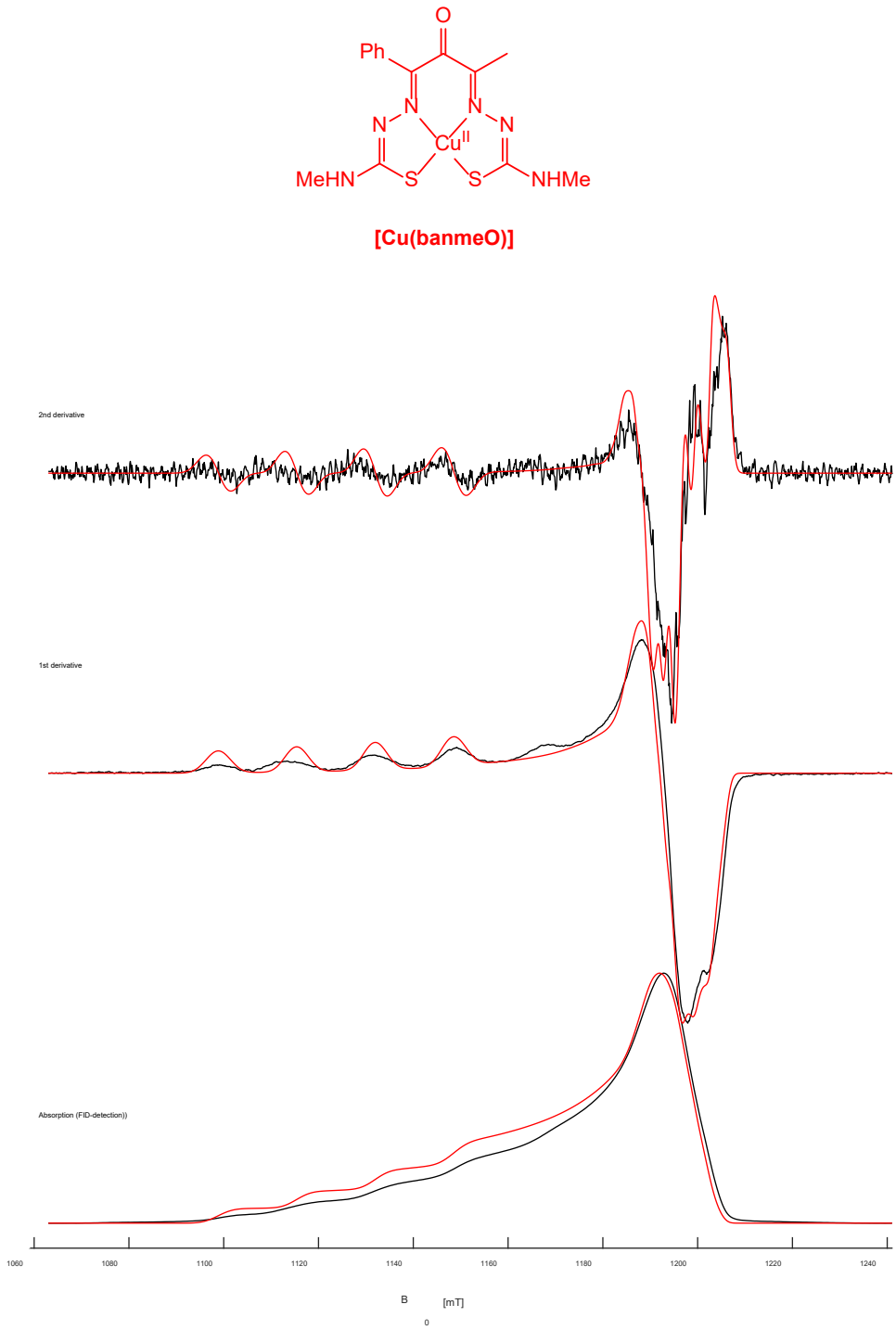

Fig. S9. Q-band FID-detect field-sweep EPR of $[Cu(banme)]^-$ (aerobic) at 30 K. Experimental (black) and simulation (red). Spin Hamiltonian parameters: g_x 2.0248, g_y 2.0357, g_z 2.158; $A_{Cu,x}$ (MHz) 79, $A_{Cu,y}$ 50, $A_{Cu,z}$ 490; $A_{N,x,y,z}$ 41.9; linewidths (x, y and z) 65, 65 and 120 MHz.

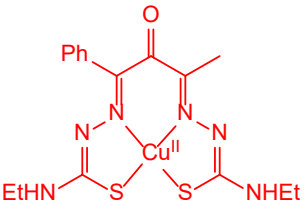

[Cu(banetO)]

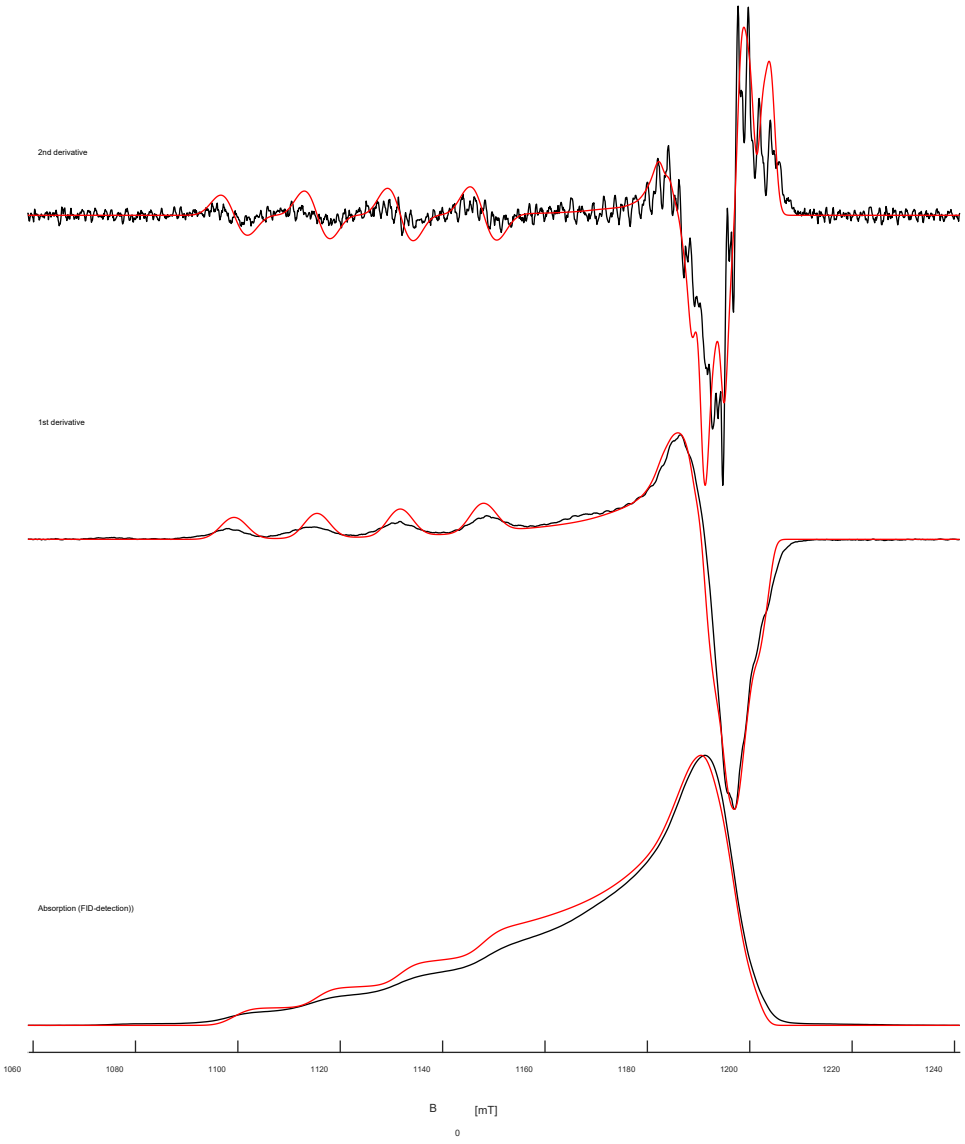

Fig. S10. Q-band FID-detect field-sweep EPR of $[Cu(banet)]^-$ (aerobic) at 30 K. Experimental (black) and simulation (red). Spin Hamiltonian parameters g_x 2.0248, g_y 2.0357, g_z 2.158; $A_{Cu,x}$ (MHz) 79, $A_{Cu,y}$ 50, $A_{Cu,z}$ 490; $A_{N,x,y,z}$ 41.9; linewidths (x, y and z) 65, 65 and 120 MHz

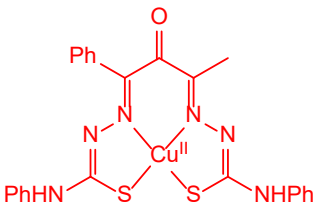

[Cu(banpheO)]

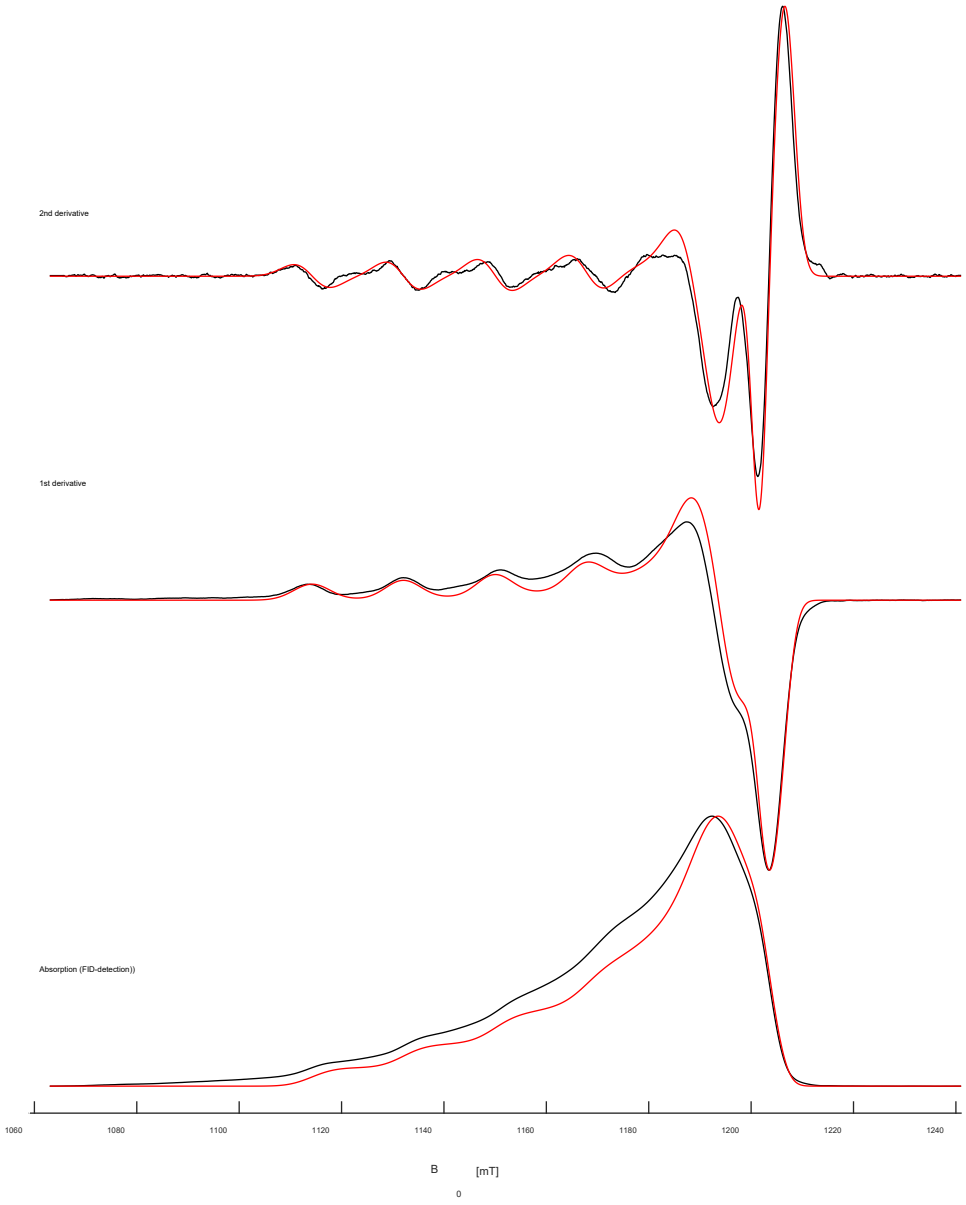

Fig. S11. Q-band FID-detect field-sweep EPR of $[Cu(banphe)]^-$ (aerobic) at 30 K. Experimental (black) and simulation (red). Spin Hamiltonian parameters g_x 2.0183, g_y 2.0377, g_z 2.1270; $A_{Cu,x}$ (MHz) 9, $A_{Cu,y}$ 34, $A_{Cu,z}$ 490; $A_{N,x,y,z}$ 41.9; linewidths (x, y and z) 65, 65 and 120 MHz.